URSI AP-RASC, Sydney, Australia, 17 – 22 August 2025

Can the DS technique help to mitigate atmospheric phase delay artifacts in ground-based SAR interferograms of natural scenes?

Fathin Nurzaman[(1)], Giovanni Nico [(2)], and Yuta Izumi[(1)]
(1) Graduate School of Engineering, Muroran Institute of Technology, Hokkaido, Japan
(2) Italy's National Research Council, Institute for Applied Mathematics "M. Picone", Bari, Italy

Abstract

In this work, we review the implementation of the Distributed Scatterer (DS) technique in the processing pipeline of ground-based Synthetic Aperture Radar (GBSAR) interferometry. DS consists of a group of pixels that individually have a low signal-to-noise ratio (SNR) but can collectively enhance SNR through statistical processing, as they are assumed to share the same underlying deformation signal. Despite its advantages, the DS-based InSAR technique has seen limited application in GBSAR due to the typically high SNR of GBSAR data and its predominant use in infrastructure monitoring with lots of already reliable scatterers. A DS-based InSAR technique adapted to GBSAR data characteristics is proposed here. The method is tested on SAR images acquired by a GBSAR system over a scene, primarily covered by rocks and bare soils, covered by short vegetation - conditions that are well-suited for DS analysis. We compare the interferograms generated using the proposed DS approach with those obtained through the conventional multi-looking method and study how they could affect the subsequent atmospheric correction process, which is a crucial step of GBSAR interferometry.

1. Introduction

Ground-Based InSAR has become an established technique for monitoring terrain and infrastructure stability (e.g. [1] and references therein). Its advantages over other techniques include sub-millimetric precision, the ability to monitor large areas, non-invasive operation, and all-weather capability.

The mitigation of atmospheric phase delay artifacts is a key problem when processing interferometric GBSAR time series. Various approaches have been proposed, including modeling in-situ meteorological measurements (e.g., [2]) and applying Persistent Scatterer (PS) techniques originally developed for processing spaceborne interferometric SAR time series [3]. The PS-based method selects pixels with high phase stability and processes only these pixels for both displacement measurement and atmospheric effect estimation. In this approach, often referred to as a data-driven method, the atmospheric effect is derived directly from the interferometric data itself.

This data-driven approach has become a staple in ground-based GB InSAR due to the nature of ground-based measurements, such as short temporal baselines and limited observation ranges, which enhance the signal-to-noise ratio (SNR) and, consequently, the availability of PS. More advanced data-driven techniques have been proposed and widely implemented, including the joint removal of topographically correlated atmospheric effects when an external Digital Elevation Model (DEM) of the scene is available [4]. Furthermore, more sophisticated data-driven approaches that operate across both spatial (within each interferogram) and temporal (long time-series) domains have also been introduced [5-6].

However, in the case of natural scenes, the application of PS technique is less effective due to the lack of strong scatterers. More importantly, the low SNR associated with the non-PS pixel would also degrade the effectiveness of the data-driven approach in the subsequent atmospheric compensation step.

In this paper, we investigate the application of the Distributed Scatterer (DS) techniques developed for the processing of spaceborne SAR data [7]. The DS-based method is used when stable scatterers are sparse, such as in natural terrain. It works by collectively processing groups of pixels with high similarity, enhancing the SNR of the underlying deformation signal. The DS-based method has rarely been applied in GB InSAR due to the inherently high SNR in GB measurements, making the PS-based approach sufficient in most cases. Additionally, GB InSAR is predominantly used for infrastructure monitoring, where PS availability is generally high due to the presence of natural or artificial high-reflection targets (e.g. [8], [9]).

In this article, we review the performance of the DS-based method for observing natural terrain using GB InSAR. The review also considers how this approach could contribute to the subsequent atmospheric compensation step, which is crucial in GB InSAR since atmospheric effects are the dominant noise source in these measurements.

3. Methodology

3.1 PS Selection for GBSAR Interferometry

DS are defined as pixels that exhibit similar temporal characteristics to nearby pixels within a specified local window. In the early development of the DS technique, pixel similarity was determined based on the amplitude time series. This approach was inspired by the earlier PS technique, which reliably identifies PS pixels with good phase stability by analyzing amplitude dispersion. The use of amplitude instead of phase was necessary due to the high sensitivity of phase data to noise, including atmospheric effects and topographic errors. Additionally, phase data can experience temporal phase wrapping, which hinders reliable stability measurements. These factors justify the application of amplitude-based methods, particularly for spaceborne SAR data.

However, in Ground-Based SAR (GBSAR), the risk of temporal phase wrapping is significantly reduced due to the short temporal baseline, which can be as brief as a few minutes. This short baseline also minimizes phase noise, including atmospheric effects. Furthermore, in GBSAR measurements, the sensor typically remains fixed in position, effectively eliminating topographic errors in the phase data. Therefore, we propose a modified DS technique that evaluates pixel similarity based on their phase time-series. Consider a stack of Single Look Complex (SLC) images containing k pixels. Each pixel is represented by a complex signal vector denoted as

$$y^T = [y(t_1), y(t_2), \dots, y(t_N)] \quad (1)$$

with N being the total number of the SLCs and t_i as the time at i-th SLC acquisition already in chronological order ($t_1 < t_2 < \cdots < t_N$). To have the desired phase time series we can first take the increment of the phase component in a daisy chain approach such as

$$\phi^T = [\phi_1, \phi_2, \dots, \phi_{N-1}], \quad (2)$$

where

$$\phi_i = \angle y(t_{i+1}) - \angle y(t_i).$$

Subsequently, the desired phase time series of each pixel, which is free from temporal phase wrap, can be generated from the cumulative summation of ϕ^T with the phase of the first SLC set to be zero, i.e. the first SLC is set as the reference. We can have the cumulated phase time-series vector expressed as

$$\Phi^T = [0, \varphi(t_2), \dots, \varphi(t_N)], \quad (4)$$

where

$$\varphi(t_i) = \sum_{i}^{N} \phi_{i-1}, \quad (5)$$

and $i \in \{2, 3, \dots, N\}$. With this procedure, Φ can be considered to be free from temporal unwrapping, considering the GBSAR short temporal baseline, and can be used for the similarity test needed to identify DS. The selection of DS pixels is performed by conducting a similarity test on Φ, comparing each pixel with all neighboring pixels within a specified window. Following [7], the similarity test is conducted using the Kolmogorov-Smirnov (KS) two-sample test. Once the test has been performed for all pixels, each pixel is assigned a value representing the number of pixels it is statistically similar to based on the KS test. A pixel is then classified as a DS pixel if the number of similar pixels exceeds a specified threshold. The set of pixels that are similar to a given pixel, based on the conducted test, will hereafter be referred to as the Spatially Homogeneous Pixels (SHP) of that pixel for clarity.

3.2 Phase Optimization of DS pixels

The phase optimization in [7] is performed using a procedure known as the Phase Triangulation Algorithm (PTA). This involves: (1) computing the temporal covariance matrix for each DS by using each corresponding SHP, and (2) optimizing the covariance matrix so that the off-diagonal elements, which represent the spatially filtered interferometric phase for all possible SLC combination pairs, remain consistent with one another. This ensures that the interferometric phase between times i and j is equal to any possible combination that should produce the i-to-j phase difference, e.g. $\phi_{i-j} = \phi_{i-m} + \phi_{m-j}$, hence the name 'triangulation. This phase inconsistency is mainly caused by the applied spatial averaging on the complex value instead of the phase data directly, especially when the phase dispersion is high. The process to average phase from the complex value was introduced in the early development of InSAR algorithm [10] and has become a staple since then due to the increased robustness towards speckle and noise. However, we can argue that for DS, the speckle has been minimized because all pixels belonging to a pixel's SHP have already passed the similarity test. Additionally, in the GBSAR case, the noise has also been reduced. Averaging directly on phase value also has the advantage of preserving spatial phase discontinuity or high spatial frequency component on the phase signal [11], which can be more likely attributed to the sought displacement signal.

In this work, we propose a phase optimization method based on direct spatial averaging of the interferometric phase at pixels within an SHP. Essentially, this approach acts as a spatially adaptive filter based on phase similarity, reducing the influence of dissimilar phases within the filtering window and minimizing bias in the final averaged result as opposed to the conventional multi-looked interferogram from the complex coherence, which takes into account all pixels in the specified window. The optimization is applied only to the phase differences between consecutive SLCs, resulting in an optimized interferometric phase for a daisy-chain network of interferograms. Not performing the triangulation such as in the aforementioned PTA is justified by the applied direct phase averaging, which removes phase inconsistency and also the short, consistent temporal baselines inherent in GBSAR acquisitions. In contrast, triangulation in spaceborne InSAR is primarily used to enhance interferometric phase quality in scenarios with long and inconsistent baselines, improving phase inversion results by increasing connectivity between acquisitions.

4. Results

4.1 DS Selection Step: Phase vs Amplitude similarity

The DS pixel set has been selected using the proposed approach, which accounts for phase time-series similarity. To highlight the advantage of using phase instead of amplitude, Figure 1 presents the time series of both phase and amplitude for all nine pixels within a 3×3 window. As expected, the amplitude time series of these pixels exhibit strong similarity (see Figure 1-(a)), primarily due to their close proximity. Performing the KS test on amplitude would likely result in all pixels being grouped into a single SHP set, which would then be used collectively in the subsequent DS operation.

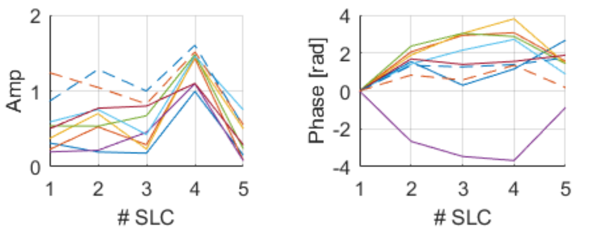

(a) (b)

Figure 1. Amplitude (a) and phase (b) time-series of a pixel group within 3 x 3 window.

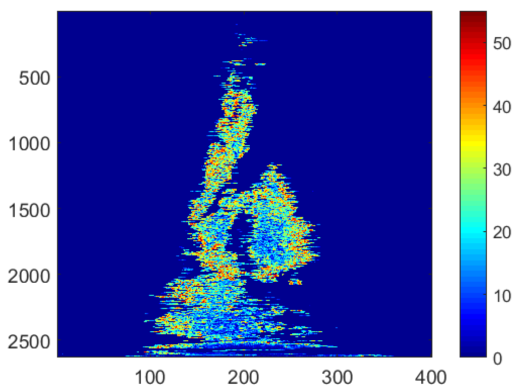

Figure 2. The amount of SHP within the search window corresponding to each pixel resulted from the proposed DS selection approach. The y-axis is the pixel number in the range direction, while the x-axis in the cross-range direction.

However, the corresponding phase time-series graph (see Figure 1-(b)) reveals that not all pixels exhibit the expected similarity. Notably, the purple line deviates significantly from the others. If this pixel were included in the SHP set, it would likely introduce bias into the final interferometry results. Therefore, performing the similarity test on the phase time-series instead is more advantageous, as it ensures that the outlier (the purple line) is excluded from the SHP set.

The result of the proposed DS method is given in Figure 2, which shows the amount of SHP in each pixel. The SHP search window size is set to 11×5 (range × cross-range), as most coherent pixels are located in areas where the pixel length in the cross-range direction is larger than the range resolution. The DS are then identified as pixels with SHP greater than 25.

4.2 Interferogram results compared with the standard multi-looking approach

The final interferogram result comprising of 5 SLCs acquisition is shown in Figure 3. This interferogram comprised 5 SLC acquisitions with a total temporal length of 75 minutes. The dense result of the DS approach allows us to see the linear phase ramping in the range direction, which is a typical characteristic of the atmospheric effect. This makes the data-driven approach for the atmospheric compensation step still a feasible option to be used hereafter.

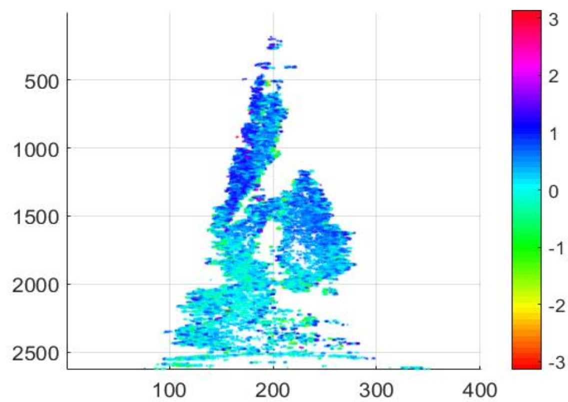

Figure 3. The final interferograms comprised 5 SLC acquisitions. The axis is set to be similar to Figure 2.

A comparison with the results obtained using conventional multi-looking, which basically a spatial boxcar filter, with the same window size, is shown in Figure 4. The interferogram being computed without applying any multi-looking is also presented (see Figure 4-(a)) to have a clear visualization of the phase variability before any spatial phase averaging. As expected, the conventional method produces a more blurred result due to the indiscriminate spatial averaging window (see Figure 4-(b)). In contrast, the DS-based approach preserves some localized or high-frequency spatial signals (see Figure 4-(c)), which is a result of DS-exclusive averaging and the averaging of phase values directly instead of the complex values. This characteristic can be beneficial in retaining localized signals, which may primarily correspond to actual deformation after the subsequent atmospheric compensation process. Since this process mainly accounts for low spatial frequency signals as atmospheric components, preserving localized signals could be advantageous.

However, given that the interferogram's temporal length is only 75 minutes, no significant displacement should have occurred. Therefore, all observed signals are likely attributable to atmospheric effects. As a result, the localized signals in Figure 4-(c) could merely be enhanced speckles, which might reduce the effectiveness of the subsequent atmospheric compensation step. More consideration should be given to the choice of window size, ensuring that it is large enough to filter out speckles but small enough to preserve the expected localized deformation signal.

5. Conclusions

In this work, we presented the results obtained by applying the DS technique to a time series of GBSAR interferograms. It has been found that the DS technique can greatly contribute to identifying stable-phase regions in GBSAR and consequently generate an interferogram with dense reliable pixels despite the lack of strong scatterers in the observed area. The technique also appears to maintain high-spatial-frequency components, which could otherwise be removed when using the general spatial filter techniques.

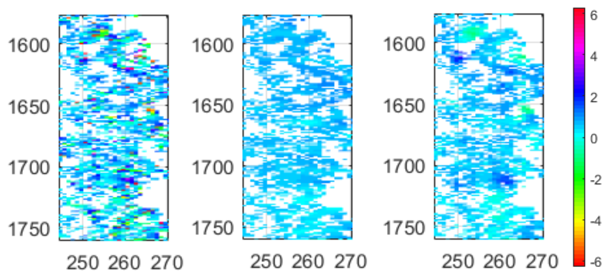

(a) (b) (c)

Figure 4. Interferograms comparison between 3 techniques: (a) Simple phase differencing with no averaging, (b) with conventional multi-looking, (c) using the proposed DS-based approach. Only showing the DS pixels for easier comparison.

References

[1] A. Anghel, M. Tudose, R. Cacoveanu, M. Datcu, G. Nico, O. Masci, A. Dongyang, W. Tian, C. Hu, Z. Ding, H. Nies, O. Loffeld, D. Atencia, S.G. Huaman, A. Medella and J. Moreira, “Compact ground-based interferometric synthetic aperture radar: short-range structural monitoring,” *IEEE Signal Processing Magazine*, **36**, 4, June 2019, pp. 42-52, doi: 10.1109/MSP.2019.2894987.

[2] L. Iannini, and A. Monti Guarnieri, “Atmospheric phase screen in ground-based radar: statistics and compensation,” *IEEE Geoscience and Remote Sensing Letters*, **8**, 3, December 2010, pp. 537-541, doi: 10.1109/LGRS.2010.2090647.

[3] L. Noferini, M. Pieraccini, D. Mecatti, G. Luzi, C. Atzeni, A. Tamburini and M. Broccolato, “Permanent scatterers analysis for atmospheric correction in ground-based SAR interferometry,” *IEEE Transactions on Geoscience and Remote Sensing*, **43**, 7, July 2005, pp. 1459-1471, doi: 10.1109/TGRS.2005.848707.

[4] R. Iglesias, X. Fabregas, A. Aguasca, J.J. Mallorqui, C. López-Martínez, J.A. Gili and J. Corominas, “Atmospheric phase screen compensation in ground-based SAR with a multiple-regression model over mountainous regions,” *IEEE Transactions on Geoscience and Remote Sensing*, **52**, 5, May 2014, pp. 2436-2449, doi: 10.1109/TGRS.2013.2261077.

[5] Y. Izumi, G. Nico, and M. Sato, “Time-series clustering methodology for estimating atmospheric phase screen in ground-based InSAR data,” *IEEE Transactions on Geoscience and Remote Sensing*, **60**, April 2021, pp. 5206309-5206309, doi: 10.1109/TGRS.2021.3072037.

[6] Y. Izumi, G. Nico, O. Frey, S. Baffelli, I. Hajnsek and M. Sato, “Kriging-based atmospheric phase screen compensation incorporating time-series similarity in ground-based radar interferometry,” *IEEE Journal of Selected Topics in Applied Earth Observations and Remote Sensing*, **17**, October 2024, pp. 17626-17636, doi: 10.1109/JSTARS.2024.3469158.

[7] A. Ferretti, A. Funagalli, F. Novali, C. Prati, F. Rocca and A. Rucci, “A new algorithm for processing interferometric Data-Stacks: SqueeSAR,” *IEEE Transactions on Geoscience and Remote Sensing*, **40**, 9, May 2011, pp. 3460-3470, doi: 10.1109/TGRS.2011.2124465.

[8] A. Di Pasquale, G. Nico, A. Pitullo and G. Prezioso, “Monitoring strategies of earth dams by ground-based radar interferometry: how to extract useful information for seismic risk assessment,” *Remote Sensing*, **18**, 1, 244, July 2018, pp. 1-27, doi: 10.3390/s18010244.

[9] G. Nico, G. Cifarelli, G. Miccoli, F. Soccodato, W. Feng, M. Sato, S. Miliziano and M. Marini, “Measurement of pier deformation patterns by ground-based SAR interferometry: application to a bollard pull trial,” *IEEE Journal of Oceanic Engineering*, **43**, 4, July 2018, pp. 822-829, doi: 10.1109/JOE.2018.2840399.

[10] D.T. Sandwell and E.J. Price, “Phase gradient approach to stacking interferograms,” *Journal of Geophysical Research*, **103,** B12, December 1998, pp. 30183–30204, doi:10.1029/1998JB900008.

[11] H. Liang, L. Zhang, X. Ding, Z. Lu, X. Li and J. Ju, "Suppression of Coherence Matrix Bias for Phase Linking and Ambiguity Detection in MTInSAR," *IEEE Transactions on Geoscience and Remote Sensing*, **59**, 2, February 2021, pp. 1263-1274, doi: 10.1109/TGRS.2020.3000991.